Korea-Australia Rheology Journal
Vol. 19, No. 3, November 2007 pp. 133-139

Structure-property relationship of melt intercalated maleated polyethylene nanocomposites

M. M. Reddy, Rahul K. Gupta, S. N. Bhattacharya, and R. Parthasarathy*
Rheology and Materials Processing Centre, School of Civil, Environmental and Chemical Engineering, RMIT University, Melbourne, Victoria 3001 Australia

(Received July 9, 2007; final revision received September 6, 2007)

Abstract

Low density polyethylene nanocomposites were prepared by melt intercalating maleic anhydride grafted polyethylene and montmorillonite clay. It has been found that maleic anhydride has promoted strong interactions between polyethylene and montmorillonite, leading to the homogeneous dispersion of clay layers. Rheological experiments revealed that prepared nanocomposites exhibited shear thinning behaviour. Polyethylene nanocomposites exhibited an increase in steady shear viscosities compared to virgin polyethylene owing to strong polymer clay interactions. The tensile strength of nanocomposites was improved but elongation at break decreased considerably. Also, barrier properties improved significantly with montmorillonite content.

Keywords : Polyethylene (PE), nanocomposoites, melt intercalation, morphology, shear viscosity

1. Introduction

Polyethylene is the highest commodity polymer consumed in the world today, with low density polyethylene (LDPE) accounting for almost 20% of polymer consumption, of which almost 40% is used in packaging applications. Very good balance of optical and mechanical properties makes it ideal for food and pharmaceutical packaging applications. However, although polyethylenes have acceptable moisture barrier characteristics, they have poor barrier characteristics to oxygen and carbon dioxide, which excludes LDPE from demanding functional packaging applications where high atmospheric tolerances are necessary.

In the last decade, there has been considerable focus, both academic and industrial, on the development of polymer nanocomposites. They exhibit dramatic enhancement of a large number of physical properties which include mechanical (Alexandre *et al.*, 2002; Sinha Ray and Okamoto, 2003) and barrier properties, flammability resistance (Gilman *et al.*, 1998), biodegradability of biodegradable polymers (Sinha Ray *et al.*, 2003), and photo oxidation rate (Tidjani and Wilkie, 2001) at very low filler content, usually below 5%.

Melt mixing is one of the widely used methods for the preparation of nanocomposites as it is a more efficient and cost effective process. Also, it is known that nanocomposite preparation requires delamination of clay and strong polymer filler interaction. Polyethylene is non-polar *i.e.* no polar groups in its back bone; thus, the homogenous dispersion of the hydrophilic silicate layers in its matrix is not possible. In general, layered silicate is modified with alkylammonium to facilitate its interaction with a polymer because alkylammonium makes the hydrophilic silicate surface organophilic. However, the organically modified silicate does not disperse well in nonpolar polypropylene or polyethylene because such nonpolar polymers have very high hydrophobicity. It was thought that *in situ* polymerization is the best way of producing polyethylene nanocomposites, until the use of modified oligomer, which can mediate the polarity between silicate layers and polymer, is realised ((Alexandre and Dubois 2000; Wang et al. 2001; Alexandre, Dubois et al. 2002; Hotta and Paul 2004; Osman and Rupp 2005).

Maleic anhydride grafted polyethylene (PE-g-MA)/clay nanocomposites were prepared using a melt intercalation technique (Wang *et al.*, 2001). The extent of exfoliation and intercalation depends completely on the hydrophilicity of the polyethylene grafted with maleic anhydride and the chain length of the organic modifier in the clay. An exfoliated nanocomposite was obtained when the number of methylene groups in the alkylamine (organic modifier) was larger than 16. This nanocomposite, with clay modified with dimethyl dihydrogenated tallow ammonium cations or octadecylammonium cations had a maleic anhydride grafting level higher than about 0.1 wt%. It is now well known that two conditions are necessary to obtain uniform

*Corresponding author: rchrp@rmit.edu.au.

dispersion of clay in the polymer matrix (Gopakumar *et al.*, 2002) *i.e.* firstly, the clay must be ion-exchanged to reduce the cohesive forces between clay platelets. Secondly, the polyolefin must be chemically modified to improve adhesion between the polymer matrix and clay filler.

In the present paper, we report results on the effect of clay loading on the rheology, mechanical and barrier properties of maleated low density polyethylene.

2. Experimental

2.1. Materials

The materials used in this investigation are: low density polyethylene (LDD203 film grade) supplied by Qenos, Australia, maleic anhydride-modified polymer (known as Fusabond MX110D) supplied by Dupont, organo-modified clay (with trade name Cloisite 15A) supplied by Southern Clay Products. Cloisite 15A is a natural montmorillonite exchanged with quaternary ammonium salt with interlayer spacing of 31.5 Å.

2.2. Preparation of Polyethylene Nanocomposites

To facilitate compatibility of LDPE with clay, LDPE was added with 5 wt% Fusabond and extruded in a Brabender twin screw extruder. The operating temperature of the extruder was maintained at 150, 155 and 170°C from hopper to die section of the extruder and the operating screw speed was maintained at 75 rpm. Maleic anhydride grafted polyethylene and clay were then mixed thoroughly and extruded again. The operating temperature of the extruder this time was maintained at 150, 160 and 170°C from hopper to die section of the extruder and the operating screw speed was maintained at 60 rpm. The total residence time of the material in the extrusion process was about 6 minutes. Nanocomposite pellets were dried at room temperature for 24 hrs before using them for film preparation. Compositions of different nanocomposites prepared in this study are shown in Table 1.

2.3. Morphological Characterization of Polyethylene Nanocomposites

The morphology of the nanocomposites was analysed using wide-angle X-ray scattering (WAXS) and transmission electron microscopy (TEM). WAXS was used to ascertain the degree of polymer chain intercalation into the clay interlayers using *d*-spacing calculation, while TEM was used to provide a pictorial interpretation of layered silicate dispersion and distribution within the polymer matrix.

Table 1. Compositions of LDPE-clay nanocomposites prepared

No	Polyethylene (Wt %)	Cloisite 15A (Wt %)
1	98	2
2	97	3
3	95	5
4	92	8

2.4. Wide Angle X-ray Scattering (WAXS)

A Philips X-ray generator set at 30 kV accelerating voltage and 30 mA current was used in WAXS analysis. Ni filtered Cu-Kα (λ=0.154 nm) radiation was used to record wide angle X-ray scattering intensities from 2θ=1.2 to 10°. The montmorillonite clay powder was mounted on a sample holder with cavity and a smooth surface was obtained by pressing the powder with a glass plate. A rotating sample holder was used in the WAXS experiment. The samples were rod-shaped having a diameter of 5 mm and a length of 15 mm. The scattering intensities were recorded and modified by subtracting background scattering measured using an empty sample holder.

2.5. Transmission Electron Microscopy (TEM)

The samples for transmission electron microscopy were prepared by sectioning the sample blocks on a RMC PowerTome *X*L ultramicrotome with a RMC CRX cryosectioning attachment. The thin sections, approximately 70-80 nm thick, were cut at −125°C with a diamond knife. The thin sections were picked up on a 300 mesh copper grid. The picked sections were stained with Ruthenium tetraoxide vapours and examined in a JEOL 100CX transmission electron microscope operated at 100 kV accelerating voltage.

2.6. Blown Film Process

An advanced extrusion blown film co-extrusion assembly manufactured by Strand Plast Maskiner, Sweden was used to prepare the nanocomposites. An outer die with 40 mm diameter and 1 mm die gap was used. Films were produced at 200°C (die exit temperature) and four different blower settings of 2.4, 2.6, 2.8 and 3.0 which correspond to average air velocities of 6.7, 7.2, 7.7 and 8.2 m/s, respectively outside the bubble. Average mass flow rate was maintained at 0.5 kg/hr in all cases. The film thickness during processing was found to vary between 60 and 80 μm. Identical processing conditions were used in blown film extrusion of all composites.

2.7. Rheology

Steady shear rheological property was measured using the Davenport capillary rheometer. A capillary rheometer usually consists of a capillary tube of uniform internal diameter, D and length, L. The fluid is driven through the capillary by a piston that is tightly fitted to the cylinder. Capillary rheometer measures the flow rate of a fixed volume of fluid through a small orifice at a controlled tem-

perature. The rate of shear can be varied by changing the capillary diameter and applied pressure. The capillary rheometer was set at 200°C. The die used was 2 mm in diameter and 32 mm in length. LDPE–clay nanocomposite pellets were poured to overfill the barrel and sufficient time was allowed to melt these pellets before the start of any measurement.

2.8. Evaluation of Mechanical Properties

Test specimens conforming to ASTM D882 were cut from the films and were subjected to tensile test in quintets on an Instron Universal Testing Machine (Model: 4467, Instron Corporation, England). Changes in the mechanical properties *i.e.* tensile strength and elongation at break were monitored. Samples with a gauge length of 100 mm and width of 10 mm were cut from the films for tensile strength measurements as per ASTM D882. The speed of stretching was 100 mm/min and the tests were conducted at room temperature. Ten samples were tested for each experiment and the average value was determined.

2.9. Barrier Properties

Oxygen transmission rates were measured using a MOCON Ox-Tran 2/21 apparatus using a mixture of air (with 50% relative humidity), and oxygen (10%) and nitrogen (90%) mixture. A constant temperature of 25°C was used. Permeation values were recorded when samples equilibrated. Seven samples were tested for each experiment and the average value was determined.

3. Results and Discussion

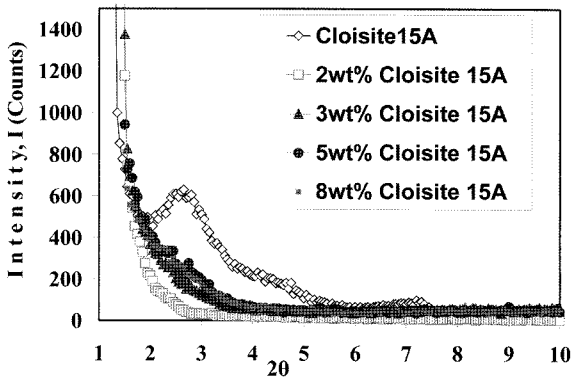

Fig. 1. XRD patterns of Cloisite 15A and LDPE/Cloisite 15A nanocomposites.

3.1. Morphology of Maleated Polyethylene Nanocomposites

The changes in the interlayer distance of clay can be identified by WAXS analysis. A shift to lower angles of the first characteristic peak represents the formation of an intercalated structure whereas the disappearance of the peak signals the probable existence of an exfoliated structure. Fig. 1 shows the XRD patterns for the Cloisite 15A and LDPE nanocomposites based on the maleated low density polyethylene with different amounts of clay loading. It can be clearly seen that Cloisite 15A leads to a peak with the d-spacing of 3.022 nm. Also, the disappearance of the peak for nanocomposites with 2, 3 and 5 wt% clay loading indicates possible exfoliation. However, for 8 wt% clay loading there is a possibility of intercalated structure

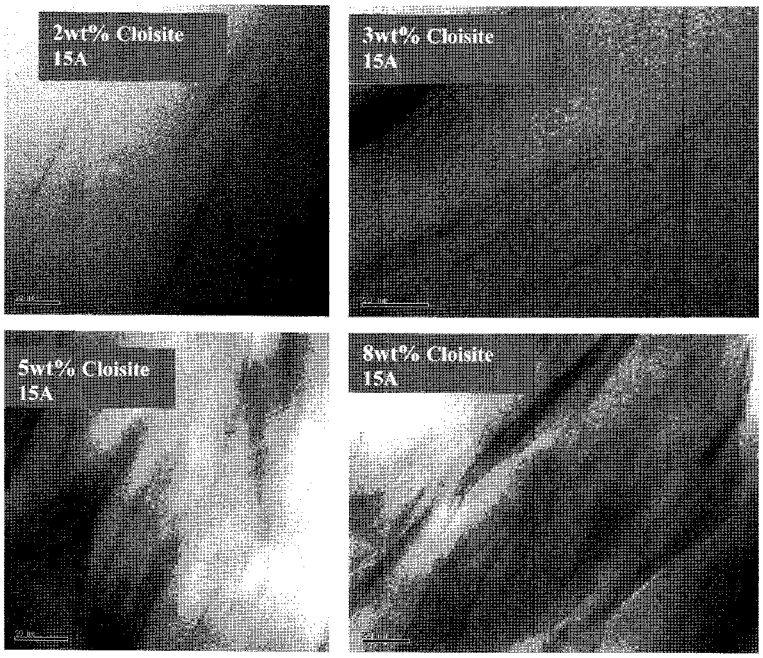

Fig. 2. TEM micrographs of LDPE/Cloisite 15A nanocomposites with different clay loading (scale 20 nm).

being present. This may be due to the fact that higher clay concentration affects the extent of exfoliation (Gopakumar *et al.*, 2002). During the melt blending of clay into polyethylene in extruder, clay particles are first fractured by mechanical shear and then polymer chains diffuse into the clay galleries because of either a physical or chemical affinity between the polymer and the organoclay surface, and push the platelets apart. Hence, an increase in clay loading leads to different morphologies due to a reduction in affinity between the polymer and clay.

The morphology of nanocomposites was further examined using TEM as it is well known that the X-ray diffraction cannot show peaks for both exfoliated and the disordered structures (Morgan and Gilman, 2003). It can be seen that the TEM images of polyethylene nanocomposites shown in Fig. 2 correspond well with the XRD patterns presented in Fig. 1. In the case of 2 and 3 wt% LDPE-clay nanocomposites, individual silicate layers are dispersed homogenously in the LDPE matrix confirming the presence of exfoliated structure. For 5 wt% LDPE nanocomposite, both individual silicate and stacked layers are present confirming the presence of mixed morphology. However, for 8 wt% clay loading, it can be seen that stacked silicate layers of about 200~400 nm length and about 50~100 nm thickness are present. The presence of stacked silicate layers substantiates the XRD results and confirms the presence of intercalated structures for 8 wt% clay loading.

3.2. Shear Rheology

Fig. 3 shows shear viscosity vs. shear rate data at 200°C for the nanocomposites used in this study. It can be seen that the addition of even small quantities of clay leads to non-Newtonian behaviour with a significant increase in shear viscosity especially at low shear rates. Power law ($\tau=K\dot{\gamma}^n$) and Ellis model ($\eta=\eta_o/1+K_1\tau^{m-1}$) were used in establishing the relationship between shear viscosity (η), shear rate ($\dot{\gamma}$) and shear stress (τ).

LDPE-clay nanocomposites with 2 and 3 wt% clay exhibit higher shear viscosity values and higher degree of shear thinning behaviour in comparison to pure LDPE (Fig. 3), which is confirmed by their lower power law index, n values shown in Table 2. The 5 and 8 wt% LDPE-clay nanocomposites also exhibit higher shear viscosity

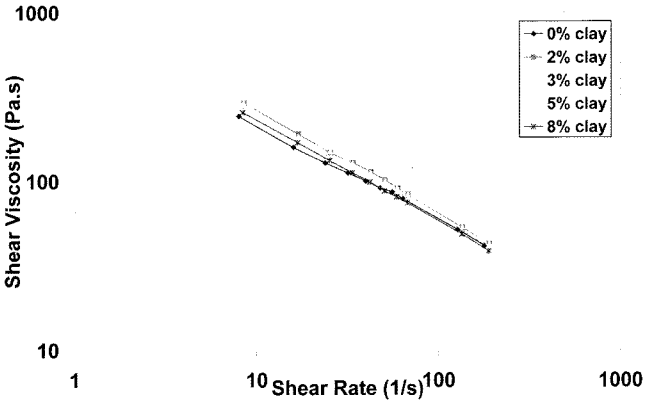

Fig. 3. Steady shear viscosity as a function of shear rate at 200°C for different LDPE-clay nanocomposite compositions.

values in comparison to pure LDPE but not as significant as those for 2 and 3 wt% nanocomposites. It has been shown in a previous research also that steady shear viscosity depends on the clay content and interaction between clay particles (Pasanovic-Zujo *et al.*, 2004).

A shear thinning fluid exhibits a plateau in its shear viscosity curve around zero and also at infinite shear rates. The zero-shear viscosity phenomenon is associated with the polymer structure and dispersions of interacting particles. The inter particle force is not strong enough to stop the deformation of the polymer which leads to the development of zero shear viscosity (Gupta *et al.*, 2006). In the present case, the zero shear viscosity is developed by the alignment of clay layers at zero shear. It increases with an increase in clay content and leads to greater interactions and therefore poor dispersion. As expected, the power law model fails to recognize the presence of zero shear viscosity of LDPE nanocomposites. Instead it predicts zero shear viscosity as infinity and infinite shear viscosity as zero. Therefore, Ellis model was chosen to represent the shear behaviour of LDPE-clay nanocomposites.

Ellis model does not predict infinite zero shear viscosity but it still predicts the other deficiency, *i.e.* zero viscosity at infinite shear rate. The three unknowns, Ellis model constant, K_1, Ellis model power index, m and zero shear viscosity, η_o were obtained through trial and error using Excel Solver tool to fit the experimental data (Table 3). Fig. 4 shows the relationship between shear viscosity (η) and

Table 2. Power law model constants (K) and index (n) for different LDPE-clay nanocomposite compositions at 200°C

Wt % clay	K	n	R^2 (Regression Coefficient)
0%	762.1	0.4458	0.9957
2%	1099.5	0.3857	0.9967
3%	1081.3	0.3888	0.9966
5%	977.3	0.3992	0.9975
8%	937.6	0.3946	0.9991

Table 3. Zero shear viscosity (η_o), Ellis model constant (K_1) and Ellis model index (m) for different LDPE-clay nanocomposite composition

	0%	2%	3%	5%	8%
η_o(Pa-s) at 200°C	16999.84	63369.26	70999.95	61117.12	50450.13
K_1	0.0124	0.0014	0.0008	0.0031	0.0018
m	2.1497	2.5232	2.6027	2.4506	2.5103

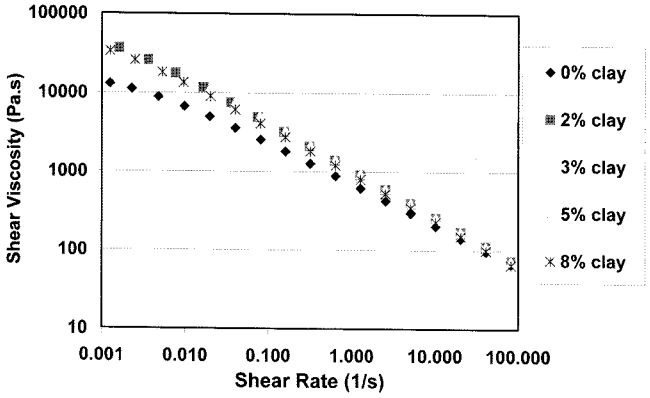

Fig. 4. Shear viscosity as a function of shear rate at 200°C for different LDPE-clay nanocomposites as predicted by Ellis Model.

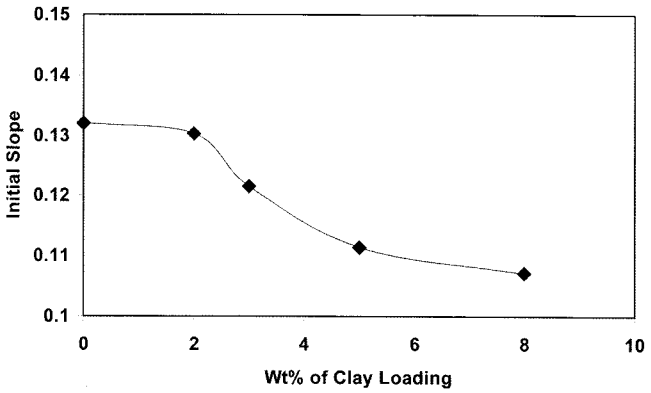

Fig. 5. Initial slope of LDPE-clay nanocomposites as a function of clay loading.

shear rate ($\dot{\gamma}$) as predicted by Ellis model. It should be noted that there is no relationship between power law index, n and Ellis model power index, (m).

From Fig. 4, it can be clearly seen that all LDPE-clay nanocomposites used in this study exhibit shear thinning behaviour, where viscosity decreases with increase in shear rate which is an indication of pseudoplastic fluid behaviour. Also, 2 and 3 wt% LDPE-clay nanocomposites exhibit the higher zero shear viscosity values as compared to pure LDPE. For the 5 and 8 wt% LDPE-Clay nanocomposites, the zero shear viscosity plateau can be hardly seen. These nanocomposites also have significantly higher zero shear viscosity values in comparison to pure LDPE but not as high as those for 2 and 3 wt% nanocomposites.

Additionally, at high shear rates ($\dot{\gamma}$ >80/s), the viscosities of the nanocomposites are comparable to that of pure LDPE. The shear viscosities exhibit rapid decrease at high shear rates. This observation suggests that the silicate layers are strongly oriented towards the flow direction at high shear rates and the shear thinning behaviour observed at these conditions is dominated by that of pure polymer (Sinha Ray and Okamoto, 2003). This also suggests that the processability of LDPE-clay nanocomposites is not greatly affected at high shear rates that are normally used for processing. Therefore, it can be concluded that LDPE-clay nanocomposites have similar ease of processability as pure LDPE and they can be processed using the usual LDPE processing techniques.

The above analysis also indicates an agreement between the rheological and morphological results. It can be seen that the 2 and 3 wt% nanocomposites which have the higher zero shear viscosity values are dominated by an exfoliated structure. On the other hand, the 5 and 8 wt% LDPE clay nanocomposites which have lower zero shear viscosity values compared to the 2 and 3 wt% samples, but still significantly higher than the pure LDPE, have a mixture of exfoliated and intercalated structure or partially disordered intercalated structure. This agrees with the findings of Xie *et al.* (2006) which showed that the final morphology of polyethylene hybrid changes from exfoliated to intercalated structure gradually with increasing clay content.

The findings from rheological and morphological results lead to the conclusion that the optimum clay content for LDPE-clay nanocomposites lies between 2 and 3 wt%. Although LDPE-clay nanocomposites with 5 and 8 wt% clay also exhibit substantially higher zero shear viscosity values in comparison to pure LDPE, the requirement of higher amount of nanoclay for their preparation make them infeasible for further processing.

Percolation threshold, which corresponds to the formation of a three-dimensional network structure whereby clay layers act as physical cross linkers hence forming a meso-structure with enhanced clay-clay interactions, is calculated for this system. The data representing the effect of clay loading on shear viscosity at low shear rates can be used to predict the percolation threshold. Fig. 5 shows Ellis slope (Initial slope), which has been determined from the plot of shear viscosity versus shear rate at low shear rates, plotted as a function of clay loading for LDPE nanocomposites. The drastic change in the slope of the curve shown in the Figure marks the percolation threshold of LDPE nanocomposites. In this case, it is around 3 wt% clay. This finding agrees well with the prior conclusion that the optimum clay content for LDPE-clay nanocomposites lies between 2 wt% and 3 wt%.

3.3. Mechanical Properties

The tensile strength and elongation at break of LDPE nanocomposites are shown as a function of clay loading in Fig. 6. Although no clear trend could be seen for tensile strength as a function of clay loading, there is a pronounced increase in tensile strength for 2 wt% clay nanocomposite. This is followed by a gradual decrease in tensile strength for 3 and 5 wt% nanocomposites. These results show that the tensile strength values for 2 and 3

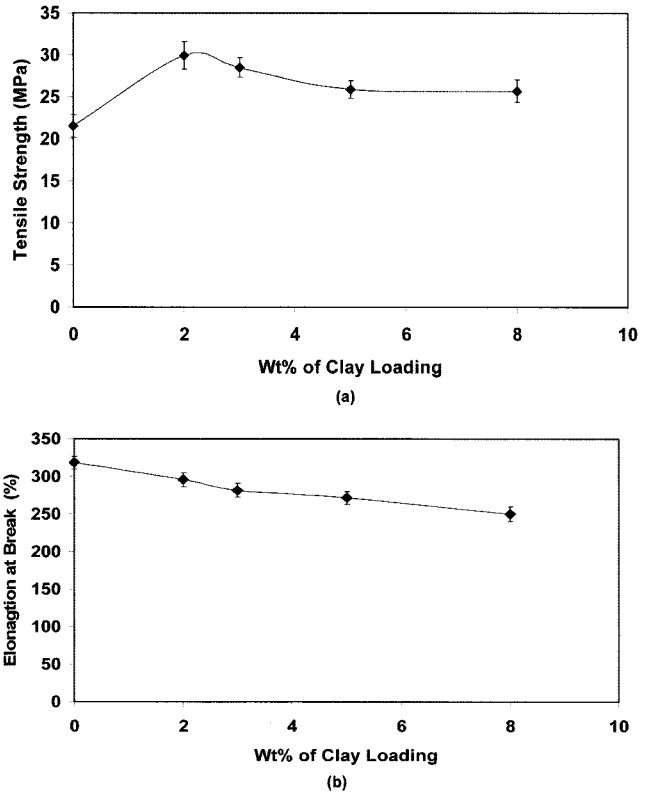

Fig. 6. Mechanical properties of the LDPE- clay nanocomposites. (a) Tensile strength (b) Elongation at break (%).

wt% nanocomposites, which have exfoliated structure, are clearly higher than those for 5 and 8 wt % nanocomposites which have dominant intercalated structure. This confirms that the essential factor that governs the enhancement of mechanical properties of LDPE-nanocomposites is the aspect ratio of clay particles (Wang *et al.*, 2002). This is due to the compatibilizing effect of maleic anhydride grafted polyethylene that improves the interfacial adhesion and leads to better stress transfer at the interface between the polyethylene matrix and clay particles (Liang *et al.*, 2004).

The elongation at break for all nanocomposite films is lower than that of virgin polyethylene. A reduction in elongation is characteristic of many filled polymer composites because the additive effectively reduces the cross-section of the polymer resisting deformation (Ji *et al.*, 2002). The polymer-filler interface often acts as a point of weakness and thus induces premature break.

To determine the percolation effect, elongation at break data is often used as a ratio of elongation at break of nanocomposite (E_C) and that of the matrix (E_M). As mentioned earlier, there is a decrease in elongation at break after the addition of small amounts of clay. The experimental data were fitted using the following equation:

$$\frac{E_C}{E_M}=b\Phi+c \quad (1)$$

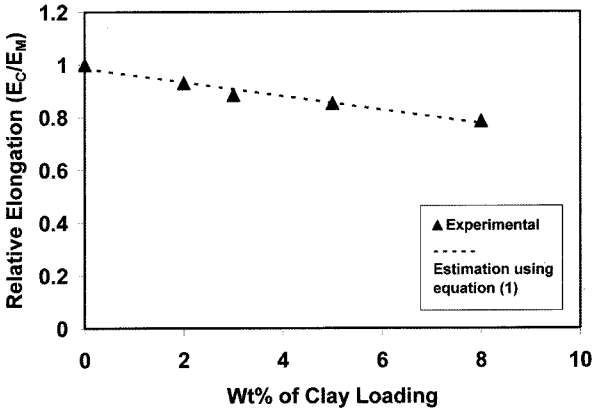

Fig. 7. Relative values of elongation at break for LDPE- clay nanocomposites as a function of the filler.

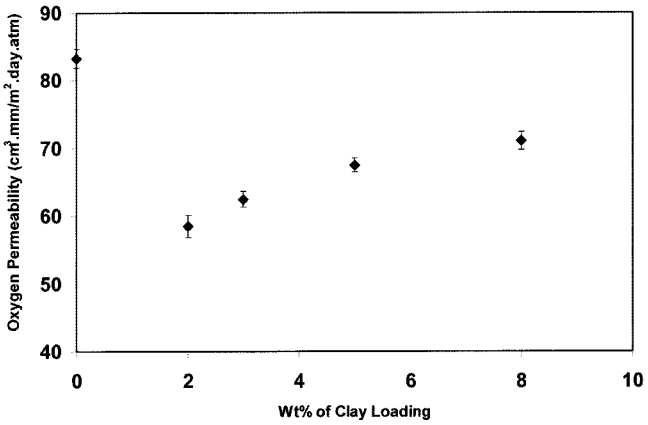

Fig. 8. Oxygen permeability properties of LDPE-clay nanocomposites as a function of the clay content.

where b and c are adjustable parameters and Φ is the weight percent of nanoclay. For the present case, b and c values are estimated to be '0.026' and '0.9841', respectively. Both experimental and calculated values are shown in Fig. 7. Since the correlation is linear, this plot cannot be used for determining the percolation threshold as was done by Chodak and Krupa (1999).

3.4. Barrier Properties

Oxygen permeation properties of LDPE nanocomposite films are shown in Fig. 8. Oxygen permeation is lower for all LDPE nanocomposite films as compared to that for the virgin LDPE film. The improvement in oxygen barrier with increase in clay loading can be attributed to the exfoliation of organoclay within the polymer matrix, which has been shown to create a more tortuous path for the gas molecules and thus more effective barrier (Jacquelot *et al.*, 2006).

4. Conclusions

Compatibilization of polyethylene by maleic anhydride

grafted polyethylene (PE-g-MA) has helped in obtaining homogenous dispersion of organomodified montmorillonite clay layers in polyethylene matrix. Rheological properties are very sensitive to the morphology obtained, *i.e.*, the strong interactions of clay layers with polyethylene lead to a significant increase in viscosity of the nanocomposites. Also, there is an increase in tensile strength with increase in clay loading for the exfoliated nanocomposites as compared to those for the intercalated nanocomposites which is a sign of improved adhesion between the polymer and clay. The same trend has been observed in barrier properties as well. Percolation threshold was calculated to determine the optimal amount of clay needed and was found to be between 2 and 3 wt% percent of clay loading.

References

Alexandre, M. and P. Dubois, 2000, Polymer-layered silicate nanocomposites: preparation, properties and uses of a new class of materials, *Materials Science and Engineering* **28(1-2)**, 1-63.

Alexandre, M., P. Dubois, T. Sun, J.M. Garces and R. Jérôme, 2002, Polyethylene-layered silicate nanocomposites prepared by the polymerization-filling technique: synthesis and mechanical properties, *Polymer* **43(8)**, 2123-2132.

Chodak, I. and I. Krupa, 1999, Percolation effect and mechanical behavior of carbon black filled polyethylene, *Journal of Materials Science Letters* **18(18)**, 1457-1459.

Gilman, J.W., T. Kashiwagi, J.E.T. Brown, S. Lomakin, E.P. Giannelis and E. Manias, 1998, Flammability studies of polymer layered silicate nanocomposites, *Materials and process affordability-Keys to the future* **1**, 1053-1066.

Gopakumar, T.G., J.A. Lee, M. Kontopoulou and J.S. Parent, 2002, Influence of clay exfoliation on the physical properties of montmorillonite/polyethylene composites, *Polymer* **43(20)**, 5483-5491.

Gupta, R.K., V. Pasanovic-Zujo and S.N. Bhattacharya, 2006, Shear and extensional rheology of EVA/layered silicate-nanocomposites, *Journal of Non-Newtonian Fluid Mechanics* **128**, 116-125.

Hotta, S. and D.R. Paul, 2004, Nanocomposites formed from linear low density polyethylene and organoclays, *Polymer* **45(22)**, 7639-7654.

Jacquelot, E., E. Espuche, J.F. Gerard, J. Duchet and P. Mazabraud, 2006, Morphology and gas barrier properties of polyethylene-based nanocomposites, *Journal of Polymer Science, Part B, Polymer Physics* **44(2)**, 431-440.

Ji, X.L., J.K. Jing, W. Jiang and B.Z. Jiang, 2002, Tensile modulus of polymer nanocomposites, *Polymer Engineering & Science* **42(5)**, 983-993.

Liang, G., J. Xu, S. Bao and W. Xu, 2004, Polyethylene/maleic anhydride grafted polyethylene/organic-montmorillonite nanocomposites. I. Preparation, microstructure, and mechanical properties, *Journal of Applied Polymer Science* **91(6)**, 3974-3980.

Morgan, A.B. and J.W. Gilman, 2003, Characterization of polymer-layered silicate(clay) nanocomposites by transmission electron microscopy and X-ray diffraction: A comparative study, *Journal of Applied Polymer Science* **87(8)**, 1329-1338.

Osman, M.A. and J.E.P. Rupp, 2005, Interfacial interactions and properties of polyethylene-layered silicate nanocomposites, *Macromolecular rapid communications* **26(11)**, 880-884.

Pasanovic-Zujo, V., R.K. Gupta and S.N. Bhattacharya, 2004, Effect of vinyl acetate content and silicate loading on EVA nanocomposites under shear and extensional flow, *Rheologica Acta* **43(2)**, 99-108.

Sinha Ray, S. and M. Okamoto, 2003, Polymer/layered silicate nanocomposites: a review from preparation to processing, *Progress in Polymer Science* **28(11)**, 1539-1641.

Sinha Ray, S., K. Yamada, M. Okamoto, A. Ogami and K. Ueda, 2003, New polylactide/layered silicate nanocomposites. 3. high-performance biodegradable materials, *Chem Mater.* **15**, 1456-1465.

Tidjani, A. and C.A. Wilkie, 2001, Photo-oxidation of polymeric-inorganic nanocomposites: chemical, thermal stability and fire retardancy investigations, *Polymer Degradation and Stability* **74(1)**, 33-37.

Wang, K.H., M.H. Choi, C.M. Koo, Y.S. Choi and I.J. Chung, 2001, Synthesis and characterization of maleated polyethylene/clay nanocomposites, *Polymer* **42(24)**, 9819-9826.

Wang, K.H., M.H. Choi, C.M. Koo, M. Xu, I.J. Chung, M.C. Jang, S.W. Choi and H.H. Song, 2002, Morphology and physical properties of polyethylene/silicate nanocomposite prepared by melt intercalation, *Journal of Polymer Science Part B Polymer Physics* **40(14)**, 1454-1463.

Xie, Y., D. Yu, J. Kong, X. Fan and W. Qiao, 2006, Study on morphology, crystallization behaviors of highly filled maleated polyethylene-layered silicate nanocomposites, *Journal of Applied Polymer Science* **100(5)**, 4004-4011.